Morphological effects on the electronic band structure of porous silicon

M. Cruz,* C. Wang, and M. R. Beltrán
Instituto de Investigaciones en Materiales, Universidad Nacional Autónoma de México, Apartado Postal 70-360, 04510, México, Distrito Federal, Mexico

J. Tagüeña-Martínez
Laboratorio de Energía Solar, Instituto de Investigaciones en Materiales, Apartado Postal 34, Código Postal 62580, Temixco, Morelos, Mexico

(Received 17 April 1995; revised manuscript received 10 August 1995)

Porous silicon presents a fascinating pore morphology, which could be relevant for its efficient luminescent properties in the visible spectrum. This work attempts to give some insight into the understanding of its optical properties, by studying the electronic band structure. The porous structure is modeled as empty columns of different sizes and shapes, produced into an otherwise perfect silicon crystal. The columns are passivated with hydrogen atoms. A tight-binding Hamiltonian on an sp^3s^* basis set is applied to supercells of 8, 32, 128, and 256 atoms. Due to the simplicity of the model, morphology effects can be analyzed in detail, even in the case where the column diameter oscillates is included. The results show that the band gap broadens and the conduction-band minimum shifts towards the Γ point, producing an almost direct band gap, as the porosity increases. A strong splitting of the originally degenerate states at the top of the valence band is also observed, for certain morphologies. Finally, the implications of quasiconfinement, where electrons can find ways out through the necks between the pores, are discussed.

I. INTRODUCTION

Efficient visible luminescence in porous silicon (PS) at room temperature has been reported in samples produced by electrochemical etching in a hydrofluoric solution.[1] This surprising optical property has stimulated great interest, since it is well known that bulk silicon has an indirect band gap of 1.1 eV, which prevents efficient interband radiative recombination in the visible region. Besides the challenge of the basic understanding of this phenomenon, PS has the technological importance of achieving all-silicon-based optoelectronic devices.

There have been different attempts to explain the light emission from PS. At the moment there are two promising models explaining the mechanisms involved in the luminescence process. One of them emphasizes the quantum confinement effect[1] and the other suggests the essential participation of the localized surface states in the silicon nanostructures.[2] Both approaches strongly depend on the geometry of the silicon skeleton created during the anodic dissolution process. The quantum confinement is not isotropic in a complex interconnected morphology and the surface curvature could affect the surface states and the charge distribution.

It is worth stressing that in spite of extensive theoretical studies,[3–9] little attention has been paid to the analysis of the PS morphology and the statistics of shapes and distribution of pores, except for simple structures such as squares and circles.[9] However, in real PS samples other types of structure coexist: wirelike, porelike, and grains or dotlike structures, depending on the preparation conditions such as temperature, acid concentration, and current intensity.[1,10] Furthermore, it is well known that changes in sample preparation leading to similar porosities but different microstructures can produce very different luminescence lines.[11,12] In what follows, we introduce a theoretical model capable of addressing this complex problem.

In Sec. II, we present some general ideas about the pore morphology of PS. In Sec. III we describe the Hamiltonian and the supercell structures used in our model. In Sec. IV we discuss the numerical results and, finally, we give the conclusions in Sec. V.

II. PORE MORPHOLOGY

We mean by pore morphology the different forms that the pores can take. When PS is prepared from a smooth sample by electrochemical etching, pores start forming from a homogeneous pattern (XY plane), because there is a random distribution of holes, and grow dendritelike, maintaining a preferential direction (z axis).[13] Transmission electron micrograph analysis reveals branching and homogeneity in the distribution of pores at different scales, i.e., a coral-like distribution at a nanometer scale and a homogeneous one at a mesoscopic scale.[1,12] The columnar diameters range from 20 to 500 Å, and their lengths are from 10 to 500 μm.[14] This difference in scale between the characteristic diameters and lengths allows us to neglect the quantum confinement in the longitudinal direction as a first approximation. However, there is experimental evidence[15] suggesting variations in the porosity along the z direction, such as variations in diameters and interconnections of wires; some of these three-dimensional facts and their effects in the electronic band structure will be analyzed.

Since the quantum confinement is mainly in the transverse plane, the third dimension (z axis) can be considered invariant in a first study. In this case, let us classify two-dimensional (2D) pores by using three parameters, if the

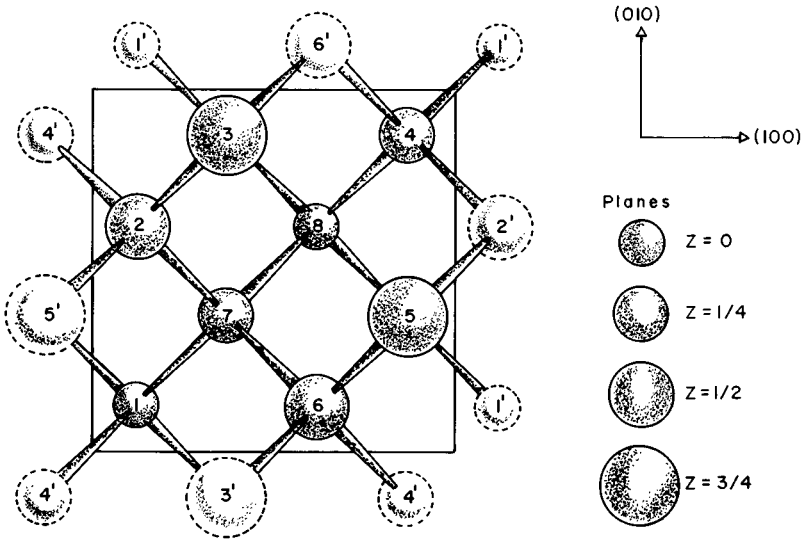

FIG. 1. Schematic representation of an 8-atom supercell used to model PS. The circle sizes indicate different planes in the z direction. The primed labels refer to periodic boundary conditions.

pore overlap is ignored. These three parameters are the porosity, the pore shape, and the distribution; the last one includes size and spatial distribution. The porosity (P) is measured as the ratio of the PS mass over the original crystalline silicon mass. The forms of the pores can be circles, squares, or more complicated shapes. Finally, the pores can be of different sizes and separated by different distances between pore centers following a given distribution. To perform a systematic study of the effects of the 2D pore on the electronic band structure, we will analyze the contribution of each one of the above parameters separately, fixing two of them.

In the case of what we call a three-dimensional (3D) pore, an extra parameter is required. This parameter characterizes pore diameter fluctuations along the z axis. As could be expected, even if the PS skeleton is wirelike, photoexcited carriers in a corrugated wire would tend to populate in thicker areas and this fact could be relevant to the photoluminescence properties.[16] Actually, this idea has earlier been suggested by Canham[17] in a model of undulating columns, where thicker and thinner areas intercalate periodically in a columnar shape. Taking into account these considerations, we will extend the 2D pore analysis to 3D pore configurations.

III. THE MODEL

In the preceding section, we have discussed some geometrical considerations of the PS pores. We now have to choose a Hamiltonian to study the electronic behavior in this material, considering the complex morphology of the pores. A possible way is to use the simplest realistic tight-binding Hamiltonian, which allows us to calculate complicated pore geometries by using large supercells. As we are interested in describing the band-structure modifications around the gap, the minimum basis capable of describing an indirect band gap along the x direction is the sp^3s^* basis. We have used the parameters of Vogl, Hjalmarson, and Dow,[18] which reproduce an 1.1-eV gap in bulk crystalline silicon.

As PS exhibits a very large surface, mainly hydrogen passivated,[1] we therefore saturate the pore surface with hydrogen atoms. We are aware that we are simplifying enormously the surface description, ignoring other possible saturators and surface reconstruction. Clearly, to study luminescence phenomena, this description is insufficient. The Si-H bond length is taken as 1.48 Å. The on-site energy of the H atom is considered to be -4.2 eV, since the free H atom energy level, -13.6 eV, is so close to the s-state energy level of a free Si atom, -13.55 eV;[19] therefore, the on-site energy of H is taken to be the same as that of silicon, as in Ref. 20. The H-Si orbital interaction parameters are taken as $ss\sigma_{\text{H-Si}} = -4.075$ eV, $sp\sigma_{\text{H-Si}} = 4.00$ eV, which are obtained by fitting the energy levels of silane.[21]

The pores in PS are modeled as empty columns in the direction [001] dug into an otherwise perfect silicon crystal, where the surface dangling bonds are saturated with hydrogen atoms. In order to analyze the effects of the pore morphology, columns of various shapes varying their distribution in supercells of different sizes are used. In Fig. 1, a supercell of 8 atoms is schematically shown. Supercells of 32 and 128 atoms are built joining, on the XY plane, 4 and 16 supercells as the one shown in Fig. 1, respectively. It is important to mention that, since the supercells are XY plane extended, removing one atom in such supercells produces one-atom columnar pores along the z direction, and these columns form a square lattice on the XY plane. The 256-atom supercell is constructed by joining two 128-atom supercells, one on top of the other, along the z direction. Periodic boundary conditions are considered in the three directions and the pores are made at the center of the supercells, for example, removing the column represented by atom 8 in Fig. 1. Special care should be taken as there is a limited number of atoms that can be removed for each supercell, beyond which the solid structure would be destroyed, where quantum confinement would be even stronger. Experimentally such a porosity limit has also been observed;[22] the value of this limit

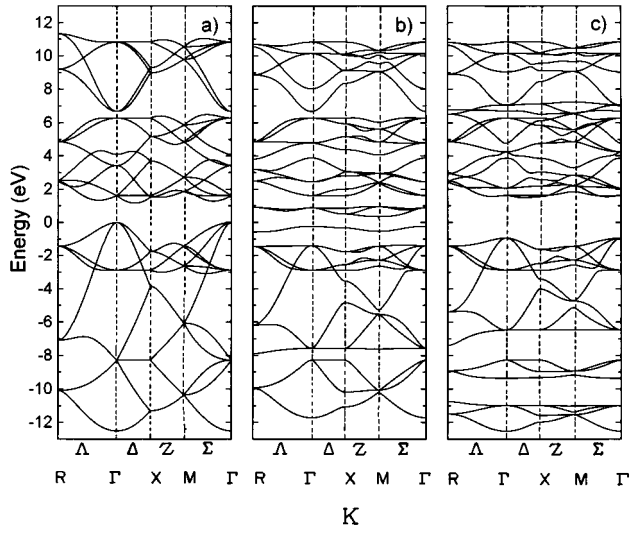

FIG. 2. Band structures for the 8-atom supercell. (a) Perfect case, (b) 1-atom pore case without saturation, and (c) saturated 1-atom pore with hydrogen atoms.

depends on the manufacturing process.

Once the Hamiltonian and the geometry are decided, we are in a position to calculate the electronic band structure of PS, diagonalizing matrices of $5n \times 5n$, where 5 is the number of orbitals considered per atom and n is the number of atoms in the supercell. This diagonalization has to be done for each $\vec{k}$ vector within the irreducible first Brillouin zone, producing a $5n$ band structure. Clearly, the supercell size is limited by the computing capabilities.

IV. RESULTS

We start by considering a 2D pore in the smallest supercell containing 8 atoms as the first step to obtain a 1-atom pore. Figures 2(a), 2(b), and 2(c) show the band structure of the 8-atom supercell when the structure is perfect, when site 8 (Fig. 1) is removed and when the four dangling bonds are saturated with hydrogen atoms, respectively. Notice that the band gap is broadened as we produce a pore structure, and that the dangling-bond states are removed from the gap when they are saturated with hydrogen atoms. The observed gap broadening is in agreement with the quantum confinement scheme.[1,3,4] It can also be seen in Fig. 2(c) that the band gap is almost direct and the degeneracy due to symmetry is broken.

As is mentioned in Sec. II, there are three possible parameters to characterize a 2D pore. Let us first consider the effects of the porosity in the electronic spectra, maintaining the pore distribution and their shapes fixed, which are chosen in this case to be squares of 1, 4, 9, 16, 25, 36, and 49 atoms removed from the center of a 128-atom supercell. Notice that in this way the distance between the pores' centers is constant. It most be pointed out that the square pores are dug in the orientation, which removes, for example, atoms 5, 6, 7, and 8 in Fig. 1, forming a 4-atom square. In Fig. 3(a) we show the variation of the conduction and the valence band borders, and in Fig. 3(b) the light-hole effective mass behavior, both plotted as a function of the porosity. Notice first that

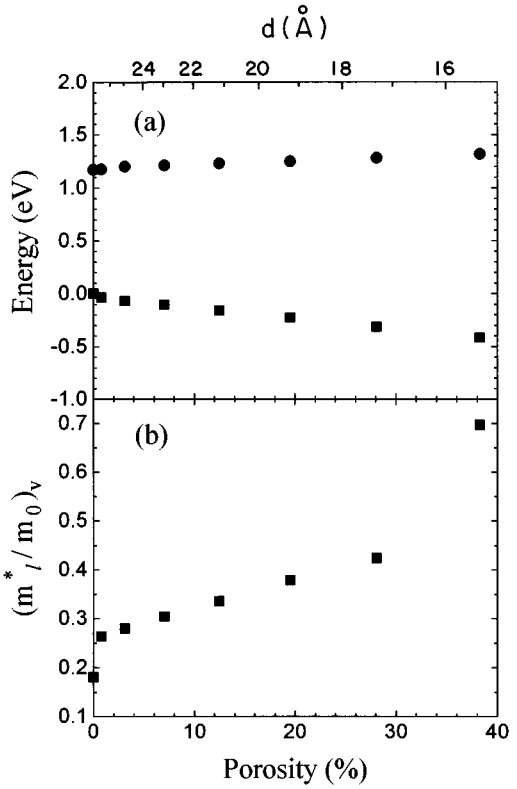

FIG. 3. (a) Shifts of the conduction and valence band borders, and (b) trend of the light-hole effective mass, both as a function of porosity for a fixed pore shape and as a function of the confinement distance (d) between pore boundaries (see Fig. 4).

the band gap broadens with the porosity; this fact is not a conventional quantum confinement effect because there are Bloch wave functions on the confinement plane. However, the electron wave functions have nodes at the pore surfaces and these extra nodes cause a sort of quantum confinement and consequently a band-gap broadening, since wave functions with wavelengths longer than the distance between nodes will not be accessible for the system. Furthermore, the band borders shift asymmetrically. That the valence band

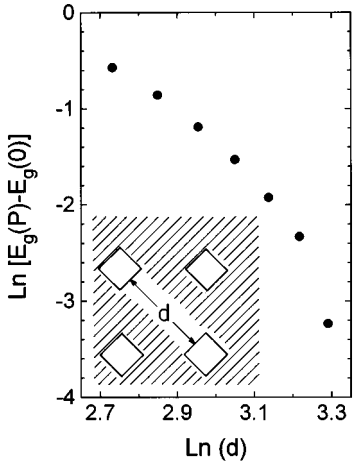

FIG. 4. Logarithmic variation in the energy gap shift with respect to the crystalline case $[E_g(0)]$ versus the distance between pore boundaries (d).

border shifts more rapidly is consistent with the difference in the band curvatures and it has already been observed.[20] The quick enlargement of the band gap observed in Fig. 3(a) seems to contradict experimental evidence,[22] where porosities as high as 79% are required before the band-gap enlargement we are predicting is observed. This apparent discrepancy can be clarified if we repeat the plot as a function of the distance between pore boundaries (confinement distance d, as shown schematically in Fig. 4), since this is a more relevant parameter for the quantum confinement and therefore, for the band-gap enlargement. It would be worth pointing out that there is not a direct relationship between the porosity and the confinement distance d, because the pore distribution could modify it. For instance, within our model, at the same porosity of 12.5% for an 8-atom supercell we have $d=3.838$ Å while, for a 128-atom supercell, $d=21.109$ Å; consequently the band-gap enlargement is totally different.

In Fig. 3(b), in spite of an expected increase of the effective mass with the porosity, there are clearly two jumps. The first occurs when the pores are introduced, which is due to the appearance of new scattering centers. The other is found at the high-porosity region of the model and is caused by the fact that we reach a percolationlike limit; i.e., pore edges almost touch each other.

Clearly, an interesting approach to analyze the energy gap behavior is plotting it *versus* the confinement distance (d) as shown in Fig. 4. A linear behavior between the gap and d in a log-log plot, expected by the effective mass theory, is not observed. However, for the high-porosity regime (small d), the slope tends to -2 in accordance with the effective mass theory. The nonlinear behavior at the low-porosity regime could be interpreted as a noncomplete or quasiquantum confinement effect, where one could define a new effective confinement distance, larger than d, obtaining in this way a -2 slope. This concept, quasiquantum confinement, means that the electrons can find ways out through the necks between the pores.

We have just seen the importance of porosity in the band gap. However, the other parameters are also relevant. The results calculated for a fixed porosity but different pore distribution are completely different. For instance, observing the case of a 1-atom pore in an 8-atom supercell and the case of a 16-atom pore (16 neighboring atoms were removed) in a 128-atom supercell, the band gap of the former case ($E_g=2.46$ eV) is much bigger than the latter one ($E_g=1.39$ eV). Clearly, in spite of having the same porosity, the quantum confinement is more intense in the first case, since the distance between pore boundaries is shorter.

Let us now, for a fixed porosity and distribution, analyze the morphology effect. We show as an example a 2-atom pore case in a 128-atom supercell. This pore can be produced in two ways, by removing (a) an atom and one next neighbor (like 7 and 8 in Fig. 1) or (b) an atom and one second neighbor (like 6 and 8 in Fig. 1). Figures 5(a) and 5(b) show the band structure for cases (a) and (b), respectively. In spite of the similarity of the results, interesting differences can be noticed. First, the band gap changes from 1.2298 eV in case (a) to 1.2478 eV in case (b). Second, although the degeneracy of the states at the top of the valence band is broken in both cases, it splits differently in each case, due to the change in the network symmetry as a consequence of the

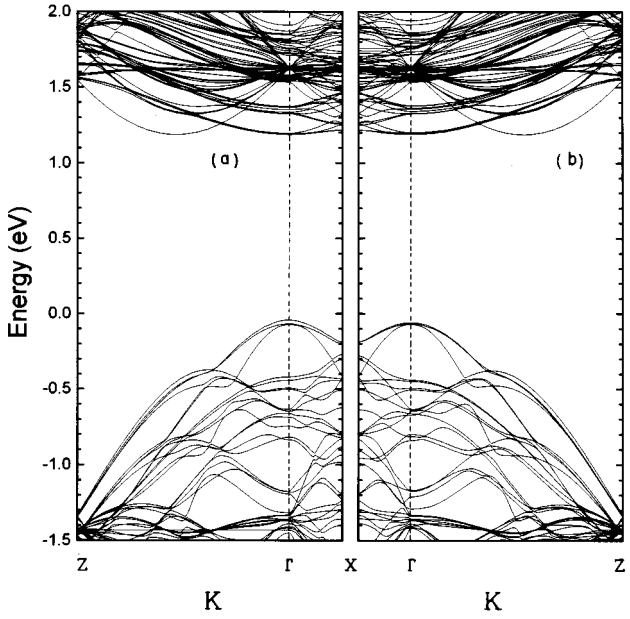

FIG. 5. Band structure around the gap for the 128-atom supercell with (a) 2-neighboring atom pore, and (b) 2-next-neighboring atom pore.

variations in the pore morphology. These differences could be important in the luminescence process; for instance, the splitting of the states at the borders could infer a double peak in the luminescence spectrum for a specific morphology of pores. It is worth mentioning that the band gaps in Fig. 5 are almost direct for supercells of 128 atoms or larger, due to the folding of the Brillouin zone. However, this is more than a simple supercell effect, since the existence of pores prevents the use of the 2-atom cell commonly used for crystalline silicon. Furthermore, PS is a *nonperiodic* homogeneous system at a mesoscopic scale and then, the periodicity of the model must tend to infinity.

Finally, we present the results for a 3D pore; i.e., the pore diameter can vary along the z direction. We have chosen the simplest geometry which consists of two alternating pores, one of 4 atoms and another of 16 atoms, producing undulating columns. In Fig. 6 we compare the band structure of a 2D pore (9-atom square pore in a 128-atom supercell) with a 3D pore (4- and 16-atom square pores in two alternating 128-atom supercells). Notice the different symmetry breaking of the states at the valence band edge. Furthermore, the 2D pore has a band gap of 1.32 eV with a porosity of 7.03%, while the 3D pore has a gap of 1.34 eV with a porosity of 7.81%. To compare the gaps at the same porosity, an interpolation procedure has been performed. The 3D band gap is 8% larger than the corresponding 2D one, which is expected due to the additional confinement in the z direction.

V. CONCLUSIONS

The importance of the morphology in a material like PS is intuitively clear but difficult to model. We have presented a new approach to study the electronic configuration of PS simple enough to be capable of studying complex morphologies. We are describing the pores as columns of different

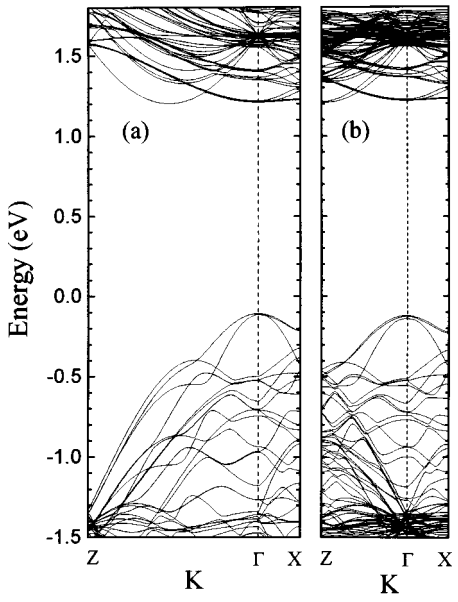

FIG. 6. Comparison of a 2D pore (9-atom square pore in a 128-atom supercell) band structure with a 3D pore (4- and 16-atom square pores in two alternating 128-atom supercells) band structure.

shapes and sizes, saturated with hydrogen atoms; although the model considers periodicity in the z direction, it is possible to introduce a periodic variation in z, producing undulating columns.

We have introduced some relevant parameters to describe the morphology effect. For the 2D pores, the porosity, the pore shape, and the distribution are considered, while for the 3D pores an additional parameter, the pore diameter fluctuation along the z axis, is required. We have analyzed the effects of each one of the above parameters, fixing the others, on the band structure. The main results are as follows:

(1) A clear broadening of the band gap due to quantum confinement.

(2) The shift of the conduction-band minimum towards the center of the Brillouin zone.

(3) The cleaning of the gap due to hydrogen surface passivation.

(4) The splitting of otherwise degenerate states at the top of the valence band for all cases.

(5) A nonlinear increase of the effective mass for both electrons and holes.

(6) An additional enhancement of the quantum confinement effect due to variations along the z direction.

All these results suggest that the quantum confinement arguments to explain the broadening of the energy gap are adequate. However, this concept should be extended to include intermediate situations, in which there are possible ''exits'' for the carriers. We are proposing to use the quasiconfinement concept to explain the jump observed in the effective mass in the high porosity regime (Fig. 3) and to understand the failure of the effective mass theory in explaining the band-gap dependence at low porosities (Fig. 4). The quantum confinement becomes complete at the limit where the pores touch each other. It is worth mentioning that the quasiconfinement is not only a peculiarity of this model, but also occurs in the real PS silicon where columns intermingle, producing alternative connections, and therefore carriers could find paths from one quantum wire to another.

The splitting of the states at the top of the valence band due to symmetry breaking is of the order of meV and, in principle, it could be studied experimentally, as has been done in other materials by optical absorption measurements at low temperatures.[23]

On the other hand, any theoretical description of the luminescent phenomena in PS would be required to include the participation of the phonon-assisted processes, since there is experimental evidence suggesting a no-direct band gap in PS.[24] These processes could be simulated by a unified model of phonon-assisted and zero-phonon radiative transitions.[25] Phonons in PS have been studied by Raman scattering, where a shift of the top optical mode towards lower frequencies has been observed.[26] The origin of this shift is similar to that of the electronic case where the valence band edge shifts towards lower energies.

Another important point is to consider disorder effects in the electronic properties of PS, since the observed band-gap enlargement[22] suggests that disorder plays an important role. This feature has been studied by Derlet, Choy, and Stoneham;[27] where, within a constant effective mass scheme, a statistical analysis of silicon crystallites is presented. They found very good agreement with experimental absorption data.[22] A similar statistical average over a pore morphology distribution could be introduced to the present model in bigger supercells. Moreover, the 3D clusterlike maximum confinement could be obtained as the limit case of the present supercell model, when a strong z-direction pore oscillation leads to almost isolated crystallites. Other saturators such as oxygen compounds can also be considered. An important improvement must be to simulate the surface more adequately, considering the variation of the tight-binding parameters close to the surface by including effects such as charge distribution, surface reconstruction, and electron-electron interactions. These extensions are currently in progress.

We would like to acknowledge enlightening discussions with Professor R.J. Elliott and Professor R.A. Barrio. We also thank Dr. T.C. Choy for the critical reading of the manuscript, pointing out the importance of disorder in PS. This work has been partially supported by Project Nos. DGAPA-IN104595-UNAM, CONACyT-4229-E, and CRAY-UNAM.

*Present address: Escuela Superior de Ingeniería Mecánica y Eléctrica-UC, IPN, Mexico.

[1] L.T. Canham, Appl. Phys. Lett. **57**, 1046 (1990); A.G. Cullis and L.T. Canham, Nature (London) **353**, 335 (1991); L.T. Canham, M.R. Houlton, W.Y. Leong, C. Pickering, and J.M. Keen, J. Appl. Phys. **70**, 422 (1991).

[2] F. Koch, in *Silicon-Based Optoelectronic Materials*, edited by M.A. Tischler, R.T. Collins, M.L. Thewalt, and G. Abstreifer,

MRS Symposia Proceedings No. 298 (Materials Research Society, Pittsburgh, 1993).
[3] F. Buda, J. Kohanoff, and M. Parrinello, Phys. Rev. Lett. **69**, 1272 (1992).
[4] A.J. Read, R.J. Needs, K.J. Nash, L.T. Canham, P.D.J. Calcott, and A. Qteish, Phys. Rev. Lett. **69**, 1232 (1992).
[5] G.D. Sanders and Y.C. Chang, Phys. Rev. B **45**, 9202 (1992); G.D. Sanders, C.J. Stanton, and Y. C. Chang, *ibid.* **48**, 11 067 (1993).
[6] G.G. Qin and Y.Q. Jia, Solid State Commun. **86**, 559 (1993).
[7] C. Delerue, G. Allan, and M. Lannoo, Phys. Rev. B **48**, 11 024 (1993).
[8] B. Delley and E.F. Steigmeier, Phys. Rev. B **47**, 1397 (1993).
[9] Jian-Bai Xia and Yia-Chung Chang, Phys. Rev. B **48**, 5179 (1993).
[10] A. Bsiesy, F. Muller, M. Ligeon, F. Gaspard, R. Herino, R. Romestein, and J.C. Vial, Phys. Rev. Lett. **71**, 637 (1993).
[11] S. Schuppler, S.L. Friedman, M.A. Marcus, D.L. Adler, Y.-H. Xie, F.M. Ross, T.D. Harris, W.L. Brown, Y.J. Chabal, L.E. Brus, and P.H. Citrin, Phys. Rev. Lett. **72**, 2648 (1994).
[12] O. Teschke, F. Alvarez, L. Tessler, and U. Kleinke, Appl. Phys. Lett. **63**, 1927 (1993); O. Teschke, M.C. Goncalves, and F. Galembeck, *ibid.* **63**, 1348 (1993).
[13] V. Lehmann, in *Light Emission from Silicon*, edited by S.S. Iyer, R.T. Collins, and L.T. Canham, MRS Symposia Proceedings No. 256 (Materials Research Society, Pittsburgh, 1992).
[14] S.F. Chuang, S.D. Collins, and R.L. Smith, Appl. Phys. Lett. **55**, 1540 (1989).
[15] P. Fauchet (private communication).
[16] Xun Wang, Daming Huang, Ling Ye, Min Yang, Pinghai Hao, Huaxiang Fu, Xiaoyuan Hou, and Xide Xie, Phys. Rev. Lett. **71**, 1265 (1993).
[17] L.T. Canham, in *Progress Towards Understanding and Exploiting The Luminescent Properties in Highly Porous Silicon*, edited by D.C. Bensahel, L.T. Canham, and S. Ossicini (Kluwer Academic Publishers, Dordrecht, 1993).
[18] P. Vogl, H.P. Hjalmarson, and J.D. Dow, J. Phys. Chem. Solids **44**, 365 (1983).
[19] Walter A. Harrison, *Electronic Structure and the Properties of Solids* (Freeman, San Francisco, 1980).
[20] Shang Yuan Ren and John D. Dow, Phys. Rev. B **45**, 6492 (1992).
[21] Fu Huaxiang, Ye Ling, and Xide Xie, Phys. Rev. B **48**, 10 978 (1993).
[22] I. Sagnes, A. Halimaoui, G. Vincent, and P.A. Badoz, Appl. Phys. Lett. **62**, 1155 (1993).
[23] O.D. Dubon, J.W. Beeman, L.M. Falicov, H.D. Fuchs, E.E. Haller, and C. Wang, Phys. Rev. Lett **72**, 2231 (1994).
[24] P.D.J. Calcott, in *Microcrystalline Semiconductors: Materials Science and Devices*, edited by P. M. Fauchet, C. C. Tsai, L. T. Canham, I. Shimizu, and Y. Aoyagi, MRS Symposia Proceedings No. 283 (Materials Research Society, Pittsburgh, 1993).
[25] M.S. Hybertsen, Phys. Rev. Lett. **72**, 1514 (1994).
[26] M. Cruz and C. Wang, Physica A **207**, 168 (1994).
[27] P.M. Derlet, T.C. Choy, and A.M. Stoneham, J. Phys. Condens. Matter **7**, 2507 (1995).